Journal of Power Sources 195 (2010) 5101–5108

Contents lists available at ScienceDirect

Journal of Power Sources

journal homepage: www.elsevier.com/locate/jpowsour

Ion transport and ion–filler-polymer interaction in poly(methyl methacrylate)-based, sodium ion conducting, gel polymer electrolytes dispersed with silica nanoparticles

Deepak Kumar, S.A. Hashmi*

Department of Physics & Astrophysics, University of Delhi, Delhi 110007, India

ARTICLE INFO

Article history:
Received 5 December 2009
Received in revised form 30 January 2010
Accepted 5 February 2010
Available online 17 February 2010

Keywords:
Gel electrolyte
Nanocomposite
Poly(methyl methacrylate)
Silica
Sodium ion conduction

ABSTRACT

Experimental studies are carried out on novel sodium ion conducting, gel polymer electrolyte nanocomposites based on poly(methyl methacrylate) (PMMA) and dispersed with silica nanoparticles. The nanocomposites are obtained in the form of free-standing transparent films.

A gel electrolyte with ~4 wt.% SiO_2 offers the maximum electrical conductivity of $\sim 3.4 \times 10^{-3}$ S cm^{-1} at ~20 °C with good mechanical, thermal and electrochemical stability. Physical characterization by X-ray diffraction, Fourier transformed infra-red and scanning electron microscopy is performed to examine ion/filler-polymer interaction and the possible changes in the texture of the host polymer due to liquid electrolyte entrapment and the dispersion of SiO_2 nanoparticles. The temperature dependence of the electrical conductivity is consistent with an Arrhenius-type relationship in the temperature range from 25 to 75 °C. Sodium ion conduction in the gel electrolyte film is confirmed from cyclic voltammetry and transport number measurements. The value of the sodium ion transport number (t_{Na^+}) of the undispersed gel electrolyte is ~0.23 and it is almost unaffected due to the dispersion of SiO_2 nanoparticles. The effect of SiO_2 dispersion on ionic conduction is described in terms of anion–filler surface interaction.

1. Introduction

Gel polymer electrolytes are materials of considerable interest worldwide, as an excellent substitute for liquid electrolytes in applications such as rechargeable batteries, supercapacitors, and other electrochemical devices [1–4]. These gel electrolytes are comprised of high dielectric constant plasticizers/solvents or their solution with different salts of lithium, sodium, etc. immobilized with a matrix of polymer host such as poly(methyl methacrylate) (PMMA), poly(vinylidene fluoride) (PVdF), poly(vinylidene fluoride-co-hexafluoropropylene) (PVdF-HFP), and poly(ethylene oxide) (PEO) [1–10]. The most advantageous features of these electrolytes are their free-standing consistency, high ionic mobility, and high concentration of charge carriers. In gel polymer electrolytes, the solvent/salt solutions are retained in a polymer matrix and contribute to the ionic conduction process, whereas the host polymer provides mechanical/dimensional stability to the gel electrolyte system [1–4].

Apart from various attractive properties, the gel polymer electrolytes suffer from few drawbacks such as (i) poor dimensional stability, (ii) interfacial instability towards cathode materials and (iii) lower liquid retention capacity. In order to improve their performance characteristics, various approaches have been adopted including the dispersion of micro- or nano-sized ceramic fillers (e.g., Al_2O_3, TiO_2, SiO_2, $BaTiO_3$, etc.) to form composite/nanocomposite gel polymer electrolytes [11–22]. Such fillers have been incorporated into gel electrolytes to preserve a porous structure that maximizes the adsorption of liquid electrolyte [23] and to reduce the risk of leakage [11,24,25].

Many research groups have reported various gel polymer electrolytes based on lithium, magnesium and zinc salts to realize their respective battery systems. Rechargeable lithium batteries suffer from some safety limitations and other problems. Thus, alternatives in the form of magnesium, zinc and sodium batteries have been reported, but not extensively studied [18,26,27]. In particular, sodium ion conducting gelled polymers may have the potential to be used as electrolytes in rechargeable sodium batteries. Sodium metal may be considered as an alternative to lithium as a negative electrode (anode) to fabricate gel polymer electrolyte based batteries due to its low cost, natural abundance, non-toxicity, low atomic mass (23.0) and high electrochemical reduction potential (−2.71 V vs. SHE) [28]. The combination of low mass and high voltage leads the possibility of employing sodium as an anode material in a rechargeable battery of high specific energy. When coupled

* Corresponding author. Tel.: +91 1127604881; fax: +91 1127667061.
E-mail address: sahashmi@physics.du.ac.in (S.A. Hashmi).

0378-7753/$ – see front matter © 2010 Elsevier B.V. All rights reserved.
doi:10.1016/j.jpowsour.2010.02.026

with an appropriate electropositive material, it would be capable of giving a cell of voltage > 2 V [28].

The main disadvantage of sodium metal as a negative electrode is its incompatibility with aqueous electrolytes, which is a potential fire hazard. All alkali metal batteries require non-aqueous electrolytes [29]. It is therefore necessary to develop high sodium ion conducting non-aqueous electrolytes suitable for the fabrication of rechargeable sodium batteries [28]. The development of sodium ion conducting, non-aqueous, gel polymer electrolyte nanocomposites should be preferred in view of their higher conductivity values, mechanical and electrochemical properties compared with liquid electrolytes and pure (undispersed) gel polymer electrolytes.

Poly (methyl methacrylate) (PMMA) has been chosen in the present work as a host polymer to prepare gel polymer electrolyte nanocomposites due to its good affinity with organic electrolytes, its amorphous nature, and its ability to exhibit high room temperature ionic conductivity values after the entrapment of liquid electrolytes [30,31]. In the present study, novel sodium ion conducting, gel polymer electrolyte nanocomposites are presented. These are comprised of a 1.0 M solution of $NaClO_4$ in ethylene carbonate (EC) and propylene carbonate (PC) immobilized in PMMA, dispersed with nano-sized fumed silica particles. In order to characterize the gel nanocomposites and to study ion transport behaviour within them, various physical techniques, have been employed, namely, X-ray diffraction (XRD), Fourier transformed infra-red (FTIR) analysis, scanning electron microscopy (SEM), thermal analysis, impedance spectroscopy, ionic conductivity versus composition and temperature, cyclic voltammetry, and transference number measurements. The nanocomposites are found to be in the form of mechanically stable, free-standing films that are suitable as electrolytes for rechargeable sodium batteries.

2. Experimental

2.1. Preparation of gel polymer electrolytes

Poly (methyl methacrylate) (PMMA, average molecular weight ~350,000), ethylene carbonate (EC), propylene carbonate (PC), sodium perchlorate ($NaClO_4$) and nano-sized fumed silica powder were obtained from Sigma–Aldrich. The EC and PC solvents, silica powder and sodium perchlorate were dried at ~100 °C for ~12 h prior to use.

In order to prepare the gel polymer electrolyte PMMA–EC–PC–$NaClO_4$ and its nanocomposite films, the following procedure was adopted. A liquid electrolyte solution of 1.0 M $NaClO_4$ in a 1:1 (volume:volume) mixture of EC and PC was first prepared by stirring the mixture thoroughly for ~8 h at room temperature. This liquid electrolyte mixture was then added to PMMA powder in glass petri-dish. A 3:1 (weight:weight) ratio of liquid electrolyte and PMMA powder was maintained. The PMMA–EC–PC–$NaClO_4$ mixture was then kept in oven at 70–80 °C for ~12 h for gelling followed by slow cooling. The gel polymer electrolyte was finally obtained in the form of a transparent free-standing film (thickness ~300 μm). To prepare the gel nanocomposites, different amounts of silica nanopowder were mixed with PMMA separately by making slurries using methanol. These slurries were subjected to proper mixing in an agate mortal and pastel, and then dried at room temperature to obtain the mixtures in powdered form. The liquid electrolyte solution was then immobilized in these powder mixtures to obtain gel polymer electrolyte nanocomposites by following the same process, mentioned above. These nanocomposites are also obtained in the form of free-standing thick films of thickness ~300–400 μm. A photograph of a typical nanocomposite film is shown in Fig. 1.

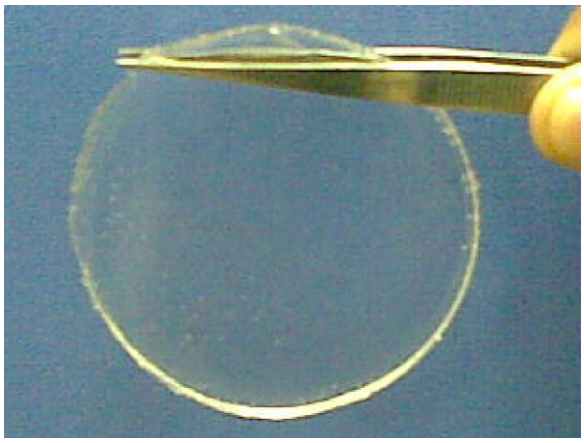

Fig. 1. Typical photograph of gel polymer electrolyte nanocomposite film EC–PC–$NaClO_4$ + PMMA dispersed with 10 wt.% SiO_2.

2.2. Instrumentation

The X-ray diffraction pattern of the gel polymer electrolyte nanocomposite films was recorded with a Philips X-ray diffractometer using Cu Kα radiation in the Bragg angle (2θ) range from 5° to 65°. FTIR spectra of the composite films were taken with the help of a PerkinElmer FTIR spectrophotometer over a wavenumber range from 400 to 4000 cm^{-1} at room temperature. The FTIR experiments were performed in a dynamic nitrogen atmosphere by averaging 16 scans per sample, keeping an optical resolution of 4 cm^{-1} for all the spectra. The morphology of the gel electrolyte films was observed by means of scanning electron microscopy (SEM) using a JEOL JSM 5600 system. The SEM measurements were performed at low vacuum after sputtering the samples with gold to prepare a conductive surface.

Thermal analysis of the gel electrolyte nanocomposites was carried out using differential scanning calorimetry (DSC). The tests were performed with a TA Instruments (Model: Q100) system in which the samples were put in a sealed aluminum pan and the measurements were carried out from −80 to 200 °C at a heating rate of 10 °C min^{-1} in a static nitrogen atmosphere. The ionic conductivity measurements of the gel electrolyte films were carried out by impedance spectroscopic analysis of a cell, in which the electrolyte films were sandwiched between two symmetrical stainless-steel (SS) electrodes. The impedance measurements were performed using a LCR Hi-Tester (HIOKI-3522-50, Japan) over the frequency range from 1 to 100 kHz with a signal level of 10 mV. The temperature dependence of the ionic conductivity was recorded over a range from 25 to 75 °C.

The total ionic transport number (t_{ion}) was evaluated using the d.c. polarization technique [32]. In this technique, a cell SS| electrolyte |SS was polarized by applying a step potential of 0.75 V and the resulting potentiostatic current was monitored as a function of time. The value of 't_{ion}' was evaluated using the formula:

$$t_{ion} = \frac{i_T - i_e}{i_T} \quad (1)$$

where i_T and i_e are total and residual current, respectively. The cationic (i.e., sodium ion) transport numbers of the gel polymer electrolyte nanocomposite films were estimated using a combination of a.c. impedance and d.c. polarization techniques, as proposed by Evans et al. [33]. Using an electrochemical analyzer (Model 608C, CH Instruments, USA), voltammetric studies were carried out to evaluate the 'electrochemical potential window' of the gel polymer electrolyte nanocomposites and to confirm their ability to conduct the sodium ions.

3. Results and discussion

3.1. Structural and morphological characterization

SEM images of the gel polymer electrolyte and its nanocomposites with silica are shown in Fig. 2. An almost flat surface is observed for the PMMA gel electrolyte. Although on careful inspection, a regular pattern of polymer alignments of 2–3 μm width, showing wave-like wrinkles, is detected (Fig. 2a). This pattern may develop due to the stress field on the polymer surface while gelling PMMA in liquid electrolyte at ~70–80 °C followed by slow cooling at room temperature. This pattern drastically changes and is distinctly observable on addition of nano-sized silica powder to the gel electrolyte (Fig. 2b and c). On dispersion of ~10 wt.% of silica nanopowder, it appears that the silica particles organize themselves in the form of highly aligned fine strands, around which the gelled polymer is wrapped. The width of these strands is about 400–500 nm. On further dispersion of silica nanopowder (~25 wt.%), the wrapping of polymeric gel around the self-organized silica becomes more prominent (Fig. 2c).

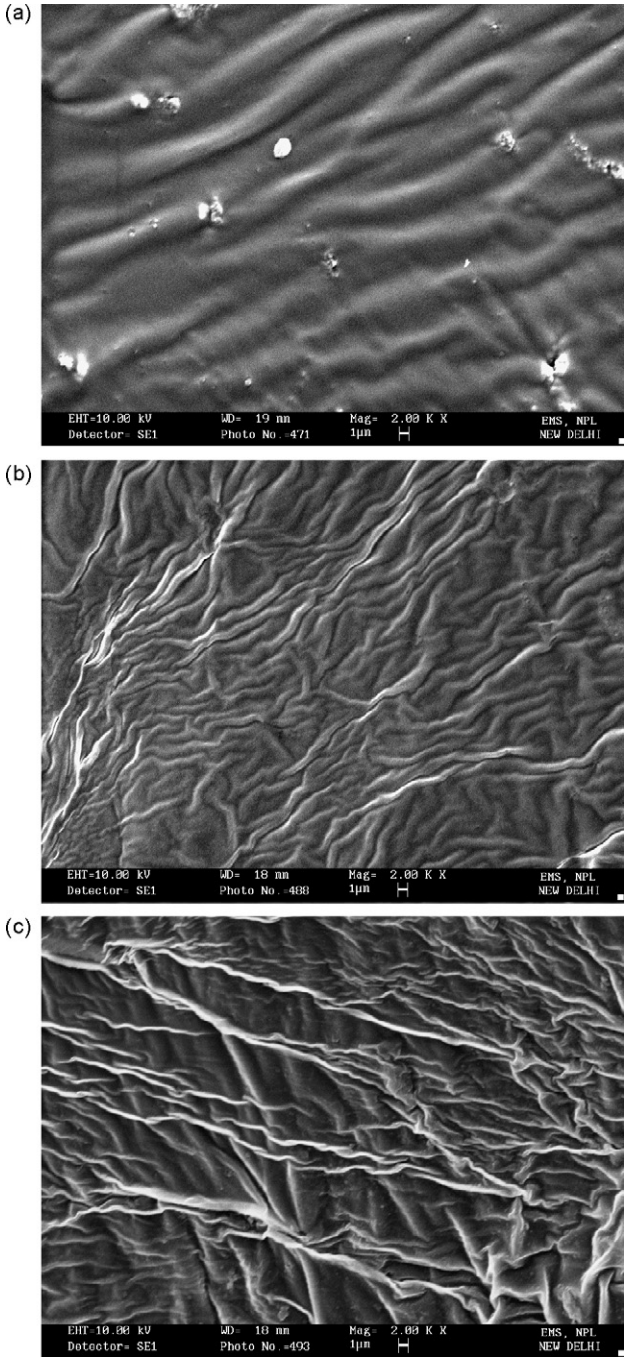

Fig. 2. SEM images of (a) EC–PC–$NaClO_4$ + PMMA gel polymer electrolyte and its nanocomposites dispersed with SiO_2 of (b) 10 wt.% and (c) 25 wt.%.

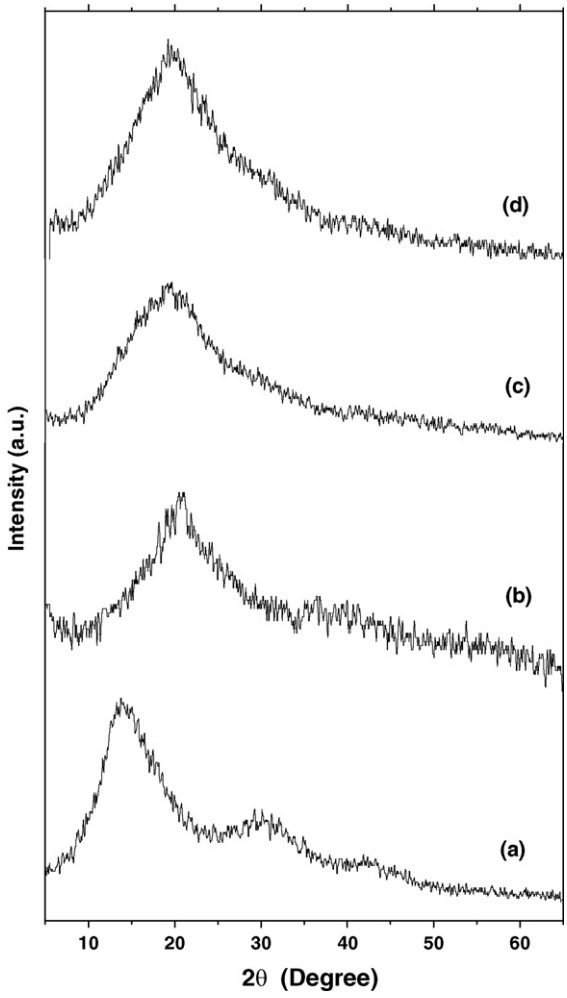

Fig. 3. XRD patterns of (a) pure PMMA, (b) EC–PC–$NaClO_4$ + PMMA gel polymer electrolyte and its nanocomposites dispersed with SiO_2 of (c) 10 wt.%, and (d) 25 wt.%.

The XRD patterns for pure PMMA, the polymer gel electrolyte and its nanocomposite films are presented in Fig. 3. The pattern for pure PMMA shows a predominant and broad peak with a maximum at 2θ ~13.8° along with broad but low-intensity peaks at 30° and 43° (Fig. 3a). These broad peaks indicate the amorphous nature of PMMA film. After immobilization of the liquid electrolyte EC–PC–$NaClO_4$, these three peaks are suppressed and a single and broad peak appears between 8° and 30° with a maximum at 19.5°. This indicates an increase in the amorphous nature of the gel polymer electrolyte. The addition of nano-sized SiO_2 particles to a gel polymer electrolyte leads to further increase in the width of the broad amorphous peak (Fig. 3c and d). Thus the addition of nano-sized SiO_2 particles may induce a significant increase in the amorphicity of nanocomposite materials.

The FTIR spectra for pure PMMA, the gel polymer electrolyte and its nanocomposites recorded for the wave number range 400 to 4000 cm^{-1} are presented in Fig. 4. A comparison of the spectra for the pure PMMA film and the gel polymer electrolyte (obtained after immobilization of liquid electrolyte EC–PC–$NaClO_4$ in PMMA

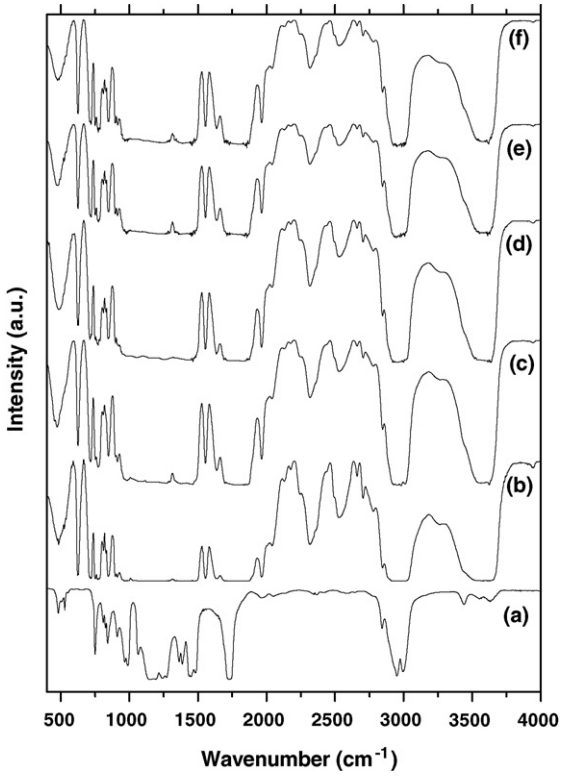

Fig. 4. FTIR spectra of (a) pure PMMA film, (b) EC–PC–$NaClO_4$ + PMMA gel polymer electrolyte and its nanocomposites dispersed with SiO_2 of (c) 5 wt.%, (d) 10 wt.%, (e) 15 wt.%, and (f) 20 wt.%.

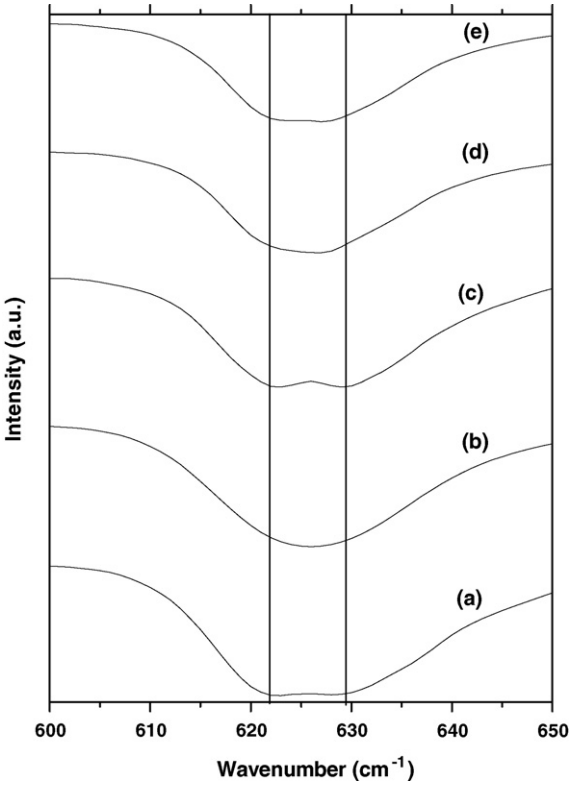

Fig. 5. Expanded representation of FTIR spectra of (a) EC–PC–$NaClO_4$ + PMMA gel polymer electrolyte and its nanocomposites dispersed with SiO_2 of (b) 5 wt.%, (c) 10 wt.%, (d) 15 wt.% and (c) 20 wt.% in 600–650 cm^{-1} spectral range.

matrix) shows almost no change in the spectral features of PMMA in terms of shifts in peak positions or peak intensities, This indicates that the bulk of liquid electrolyte is trapped in the swollen polymer matrix without showing any significant ion–polymer interaction. On dispersion of SiO_2 nanoparticles, significant changes in the spectral features in terms of the appearance of new peaks and the disappearance of existing peaks are not observed. This shows that the SiO_2 nanoparticles are present in the gel electrolyte matrix as a separate phase. On close inspection, however, the band in the region 600–650 cm^{-1} corresponding to υ_4 (ClO_4^-) is found to be affected due to the dispersion of SiO_2 nanoparticles, as shown in the expanded representation of the spectra (Fig. 5). The υ_4 (ClO_4^-) is well-separated into two peaks at 622 and 629 cm^{-1} for the undispersed gel polymer electrolyte (Fig. 5a). The appearance of the two peaks indicates the presence of two types of ClO_4^- anion. The peak corresponding to band position ~622 cm^{-1} is attributed to free anions and that at ~629 cm^{-1} to paired anions. For quantitative estimation of the fraction of these free anions and ion pairs, the corresponding spectra of the gel nanocomposites with different SiO_2 contents have been de-convoluted and two distinct peaks have been obtained. A typical de-convoluted spectral pattern is shown in Fig. 6 for a gel nanocomposite dispersed with 10 wt.% SiO_2. The fraction of free anions and ion pairs is calculated as the ratio of the area of the peak attributed to free anions and ion pairs to the total area under the υ_4 (ClO_4^-) envelope. The variation in the fraction of free anions and ion pairs as a function of the concentration of the filler SiO_2 nanoparticles in the EC–PC–$NaClO_4$ + PMMA system is presented in Fig. 7. The fraction of 'free anions' increases initially with the addition of even a very small quantity of filler nanoparticles and shows a maximum at ~5 wt.%, followed by a downward trend. Another maximum appears at ~10 wt.% of filler particles, followed by a decreasing trend. It may be noted that the variation of the fraction of ion pairs as a function of filler concentration shows a minimum corresponding to each maximum in the free anions vs. composition plots. Such variations of free and paired anions have been reported earlier in PEO-based solvent-free polymer electrolyte composites [34]. An initial addition of SiO_2 nanoparticles (4–5 wt.%) leads to the dissociation of undissociated salt/ion aggregates into free ions (anions) in the gel polymer matrix. A greater number of free anions, generated due to the addition of a greater amount of SiO_2 nanoparticles, have the tendency of ion association/pairing with cations. Hence, a decrease in free anions has been observed after the first maximum. The second maximum is related with the composite effect on the further addition of SiO_2 nanoparticles and is explained on the basis of the formation of space-charge

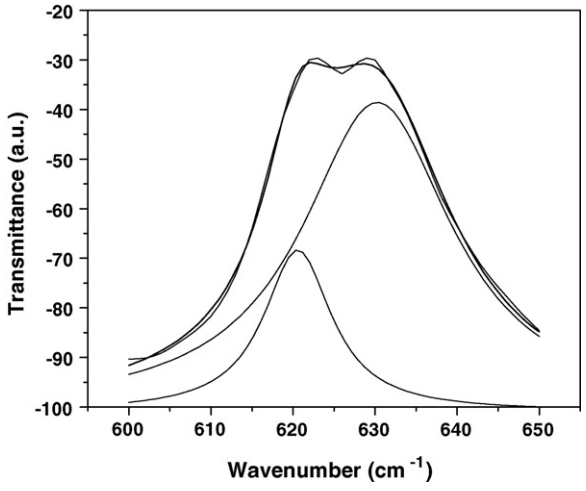

Fig. 6. Typical lorentzian fit and its de-convoluted spectral pattern for nanocomposite EC–PC–$NaClO_4$ + PMMA dispersed with 10 wt.% SiO_2 nanoparticles.

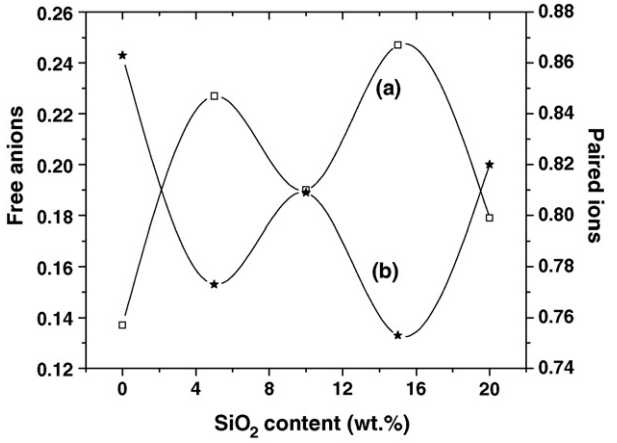

Fig. 7. Variation of fraction of (a) free anions (ClO_4^-) and (b) ion pairs with respect to dispersion of SiO_2 nanoparticles.

double-layers between fillers and the conducting gel polymer electrolyte [15,16]. Such effect predominantly occurs in the diffuse layer of the space-charge region, which can be quantitatively estimated in terms of zeta potential [35]. The SiO_2 particles, being acidic in nature, provide sites for anions (ClO_4^- ions in the present case). Hence, there is a possibility of the following reversible reaction:

$$SiO_2 + ClO_4^- \leftrightarrow SiO_2 : ClO_4^- \quad (2)$$

The SiO_2:ClO_4^- species form space-charge regions and induce a local electric field. This local electric field has the possibility to dissociate the salts/ion aggregates further and enhance the number of free anions. The decrease in number of anions after the second maximum is again due to possible ion association, or the formation of multiplets/aggregates. These interactions play a crucial role in governing the ion conduction behaviour in the gel polymer electrolyte nanocomposites. The local electric field due to the space-charge regions will also enhance the mobility of conducting ions in the composite material, as discussed later in Section 3.3.

3.2. Thermal studies

Thermal studies of the gel polymer electrolyte and its nanocomposites were performed using differential scanning calorimetry (DSC); the thermograms are shown in Fig. 8.

The glass-transition temperature (T_g) of pure PMMA film is ~127 °C. PMMA is a thermoset polymer with a backbone that is not very flexible and hence its T_g value lies at a higher temperature range. After immobilization of ~70 wt.% of liquid electrolyte EC–PC–$NaClO_4$ in PMMA, the gel polymer electrolyte film becomes highly flexible, which indicates the high flexibility of the polymeric chain backbone and hence a drastic lowering in T_g value is expected. In the present case, no characteristics of glass transition in the DSC curve of the gel polymer electrolyte have been observed between −80 and 200 °C, which indicates the possible lowering of the T_g value to below −80 °C. The glass-transition feature is also not observed in the above temperature range for gel polymer electrolyte nanocomposites (Fig. 8c and d).

Further, the onset of endothermic peak occurs at ~145 °C (Fig. 8b) and is attributed to the decomposition of electrolyte, which is possible due to fast evolution of the EC–PC mixture. This feature of EC–PC evolution has also been observed for silica-dispersed nanocomposites (Fig. 8c and d). An interesting aspect is that these electrolyte films remain stable in the gel-phase over a substantially wide temperature range of −80 to 140 °C (showing featureless DSC curves), which is advantageous for their potential application in electrochemical devices, e.g., rechargeable sodium batteries.

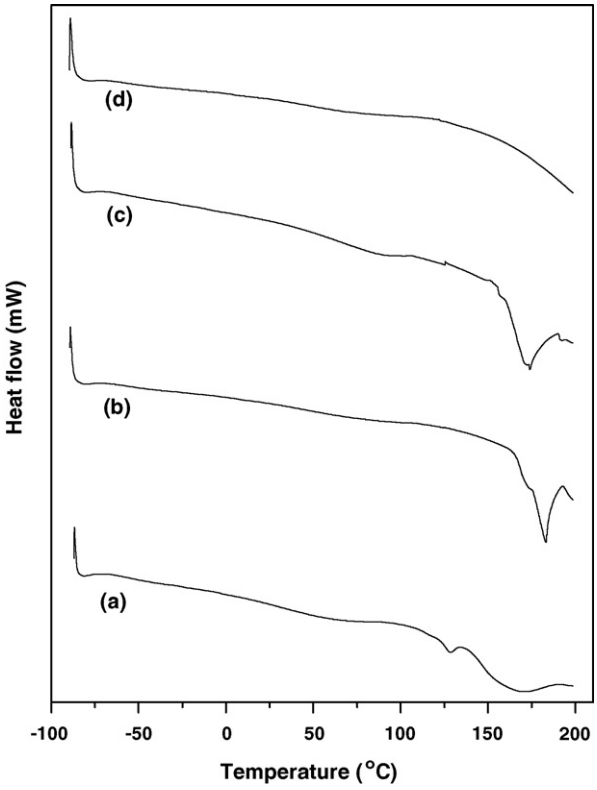

Fig. 8. DSC curves of (a) pure PMMA, (b) EC–PC–$NaClO_4$ + PMMA gel polymer electrolyte and its nanocomposites dispersed with nano-sized SiO_2 of (c) 10 wt.% and (d) 20 wt.%.

3.3. Electrical conductivity

The electrical conductivity of a liquid electrolyte, i.e., 1.0 M $NaClO_4$ solution in a EC–PC mixture, has been found to be $\sim 9 \times 10^{-3}$ S cm^{-1} at room temperature (~30 °C). After immobilization of the liquid electrolyte in ~25 wt.% PMMA, the gel polymer film offers a conductivity of 4.3×10^{-4} S cm^{-1}. The variation in electrical conductivity of the gel electrolyte system EC–PC–$NaClO_4$ + PMMA, when different amounts of silica nanoparticles are dispersed, is shown in Fig. 9. There is an initial sudden increase by almost one order of conductivity on the dispersion of SiO_2 nanoparticles, followed by two maxima at ~4 and 10 wt.%

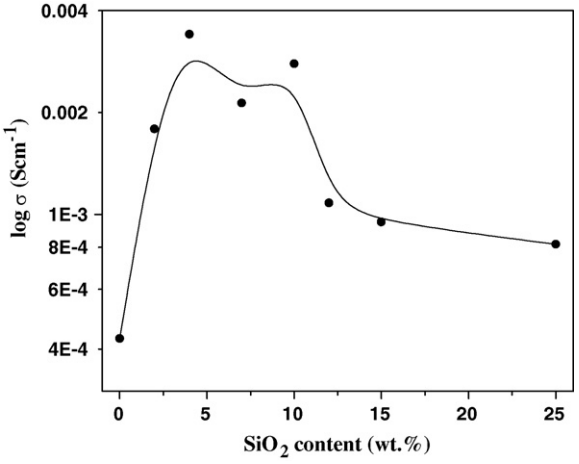

Fig. 9. Variation of room temperature electrical conductivity of gel polymer electrolyte nanocomposite films as function of nano-sized SiO_2 content.

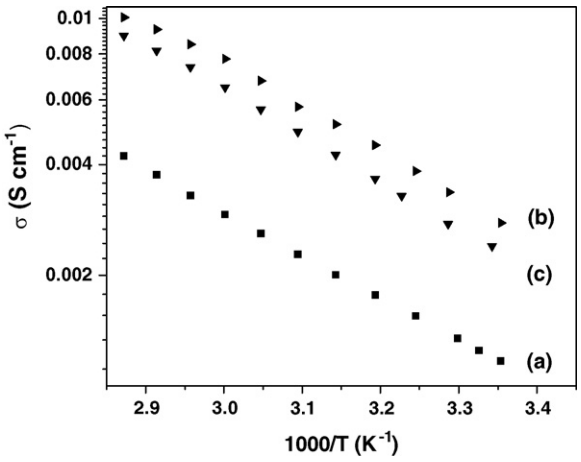

Fig. 10. Temperature dependence of electric conductivity of (a) EC–PC–$NaClO_4$ + PMMA gel polymer electrolyte and its nanocomposites dispersed with SiO_2 of (b) 10 wt.% and (c) 25 wt.%.

of SiO_2. The conductivity decreases on further addition of silica nanoparticles (Fig. 9). Two such maxima feature in the conductivity variation with respect to filler content for gel polymer electrolyte composites [18,36] and solvent-free polymer electrolytes [37–39] have been reported. A maximum conductivity of 3.4×10^{-3} S cm^{-1} is observed for the gel polymer electrolyte nanocomposite dispersed with ~4 wt.% SiO_2 nanopowder. It may be noted that a gel nanocomposite with even ~25 wt.% of SiO_2 offers a conductivity of 8.2×10^{-4} S cm^{-1}, which is higher than that for an undispersed gel polymer electrolyte. Such higher values of conductivity are attributed to the higher amorphicity of the materials and space-charge defects generated around SiO_2 nanoparticles in the polymer matrix.

The two-maximum pattern in the conductivity variation can be correlated with the variation of free anions/ion pairs (Fig. 7), as observed in the FTIR studies discussed above. The first conductivity maximum, which is observed at a lower content (4–5 wt.%) of SiO_2 nanoparticles, is associated with the generation of free ions followed by their pairing/re-association. The second conductivity maximum is related to the composite effect and is explained on the basis of the formation of a high conducting interfacial layer between the SiO_2 nanoparticles and gel polymer electrolyte due to the instantaneous presence of SiO_2:ClO_4^- species. As discussed above, such charged layers (which induce a local electric field) are responsible for the generation of free ions for conduction and their mobility, and hence enhance the overall electrical conductivity. There are two possible reasons increased for the decrease in conductivity after attaining the second maximum. The space-charge layer may cause a blocking effect at high concentrations of SiO_2 particles, which hinders the motion of mobile ions [15,16]. The another possibility is that the free ions, generated under the influence of a local electric field, may be re-associated to form ion pairs or multiplets/aggregates, and hence the number of free ions for conduction may be reduced.

The temperature dependence of the electrical conductivity of the gel polymer electrolyte and its nanocomposite films is presented in Fig. 10. In general, the σ vs. $1/T$ plots for flexible gel polymer electrolytes show the variation to have a curved nature in a wider temperature range, the behaviour is well described by the non-Arrhenius Vogel–Tammen–Fulcher (VTF) equation [40]. Whereas, in the present case of PMMA-based gel nanocomposites, almost linear σ vs. $1/T$ plots are observed from 25 to 75 °C. This linear relationship can be well represented by the Arrhenius equation:

$$\sigma = \sigma_0 \exp\left(\frac{-E_a}{kT}\right) \quad (3)$$

where σ_0 is pre-exponential factor, E_a is activation energy; k is the Boltzmann constant. The parameters have been evaluated and listed in Table 1. The sodium ion conducting gel electrolyte nanocomposite EC–PC–$NaClO_4$ + 25 wt.% PMMA + 10 wt.% SiO_2, whose composition is optimized in term of conductivity and mechanical integrity, has an electrical conductivity of the order of 10^{-3} S cm^{-1} at room temperature and 10^{-2} S cm^{-1} at 75 °C. These conductivity values indicate that the nanocomposites are promising materials for potential application in, for example, sodium batteries over a substantially wider temperature range.

Table 1
Fitting parameters for gel electrolyte and gel electrolyte nanocomposites.

SiO_2 content in gel polymer electrolyte (wt.%)	Parameters	
	E_a (eV)	σ_0 (S cm^{-1})
0	0.23	8.3×10^0
10	0.24	2.7×10^1
25	0.25	3.7×10^1

3.4. Electrochemical studies

The electrochemical potential window, i.e., working voltage range, for electrolytes is an important parameter to be evaluated from their application point of view in ionic devices such as batteries, supercapacitors, and other electrochemical devices. The working voltage range for the gel polymer electrolyte nanocomposite was evaluated by cyclic voltammetry using stainless-steel electrodes. Fig. 11 shows the typical cyclic voltammogram of the optimized electrolyte EC–PC–$NaClO_4$ + 25 wt.% PMMA dispersed with 10 wt.% SiO_2. The electrochemical stability is in the range from about −2.5 to 2.5 V (i.e., a potential window of ~5.0 V), which is an acceptable working voltage range for device applications, particularly as an electrolyte in sodium rechargeable batteries.

To confirm sodium ion conduction in the gel nanocomposite, cyclic voltammetry was performed on the symmetric cell: Na–Hg| gel electrolyte nanocomposite |Na–Hg (Na–Hg being amalgam of sodium and mercury). A typical voltammogram, in which reversible cathodic and anodic peaks are observed, is given in Fig. 12(b). No such peaks in current are given by the SS| gel elec-

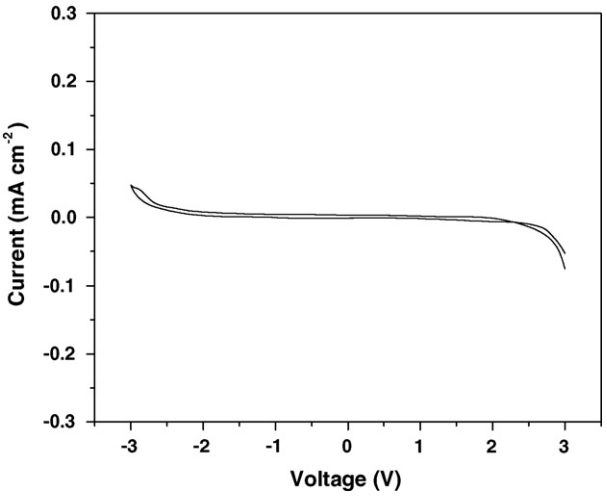

Fig. 11. Cyclic voltammogram of gel polymer electrolyte nanocomposite, EC–PC–$NaClO_4$ + PMMA dispersed with 10 wt.% SiO_2 using SS|electrolyte|SS cell at scan rate of 5 mV s^{-1}.

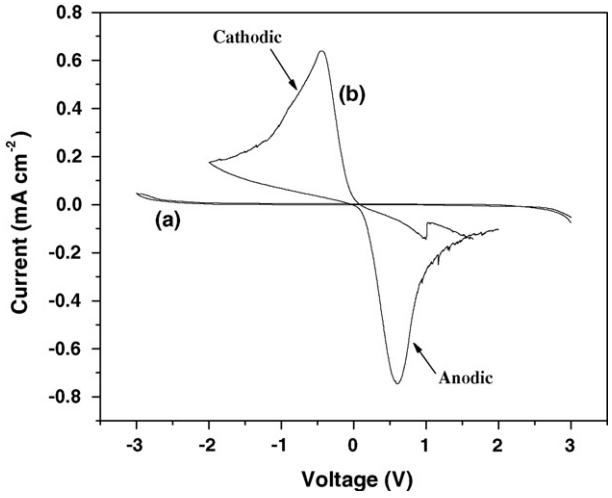

Fig. 12. Comparative cyclic voltammograms of cells: (a) SS|gel electrolyte|SS and (b) Na–Hg|gel electrolyte|Na–Hg; recorded at room temperature at scan rate of 5 mV s^{-1}. Typical gel electrolyte was PMMA + (EC + PC + 1 M $NaClO_4$) + 10 wt.% SiO_2 nanocomposite.

trolyte nanocomposite |SS cell (Fig. 12a). These cathodic and anodic peaks are attributed to highly reversible sodium plating/stripping at the sodium|gel nanocomposite interface. This suggests that the cathodic deposition and anodic oxidation of sodium are facile at the Na|gel nanocomposite interface and hence it is indicative of Na^+ ion conduction in the gel polymer nanocomposite film.

3.5. Transport number

The total ionic (cationic and anionic) transport number (t_{ion}) has been evaluated using d.c. polarization technique, as described in Section 2. The variation of current with time for a typical gel nanocomposite, EC–PC–$NaClO_4$ + 25 wt.% PMMA + 10 wt.% SiO_2, is presented in Fig. 13. The value of t_{ion} is evaluated using Eq. (1) and found to be ~0.99. The variation of current and the value of the transport number indicate that the total conductivity is predominantly ionic. It may be noted that in gel polymer electrolytes or their nanocomposites, liquid-like ion transport takes place and hence no electronic transport is expected in such electrolytes.

In general, both cationic and anionic motions contribute significantly to the total ionic transport number in the liquid or polymer

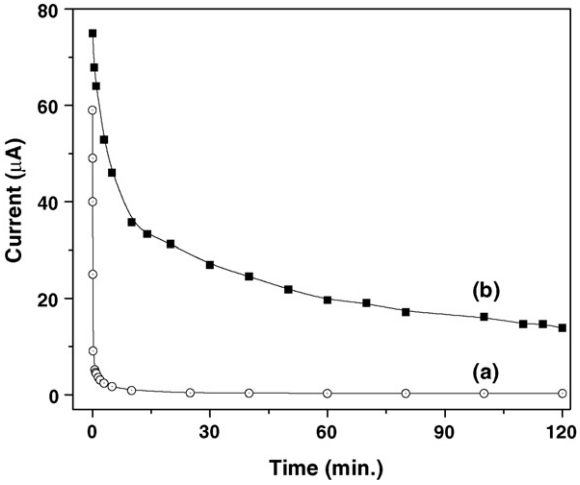

Fig. 13. d.c. polarization curves of symmetric cells : (a) SS|gel nanocomposite |SS with applied voltage of 0.75 V; (b) Na–Hg|gel nanocomposite |Na–Hg with applied voltage of 20 mV, recorded at room temperature.

Table 2
Na^+ ion transport number of gel polymer electrolyte containing different amounts of SiO_2 nanoparticles.

SiO_2 content in gel polymer electrolyte (wt.%)	Na^+ transport number
0	0.23 ± 0.02
5	0.22 ± .0.02
10	0.25 ± 0.02
15	0.28 ± 0.02
25	0.18 ± 0.02

or gelled polymer electrolytes. Hence, the cationic (Na^+ ion in the present case) transport number is an important parameter and has been evaluated by means of a combined a.c. and d.c. techniques as proposed by Evans et al. [33]. According to this technique, Na–Hg|gel nanocomposites|Na–Hg cells are polarized by applying a voltage, ΔV = 20 mV, for 2 h. The initial and final currents are subsequently recorded. Further, as a part of the method, the cells are subjected to a.c. impedance measurements prior to and after the polarization, and the values of the electrode–electrolyte contact resistances are estimated from the impedance plots. The sodium ion transport values (t_{Na^+}) are calculated by using the expression:

$$t_{Na^+} = \frac{I_s(\Delta V - R_0 I_0)}{I_0(\Delta V - R_s I_s)} \quad (4)$$

where I_0 and I_S are the initial and final current; R_0 and R_S are the cell resistance before and after polarization. The substantially higher value of residual current (I_s) indicates the reversible nature of the Na–Hg amalgam electrodes for the gel nanocomposites and further confirms Na^+ ion conduction in the material. The values of t_{Na^+}, evaluated at room temperature for gel polymer electrolyte films with different amounts of SiO_2 nanoparticles, are listed in Table 2. There is a slight enhancement in the Na^+ ion transport number with increase in the amount of SiO_2 nanoparticles for ~15 wt.% dispersion. Thereafter, the t_{Na^+} value decreases slightly on further addition of SiO_2 particles to the gel system (Table 2). It may be noted that in the same range of SiO_2 dispersion, there is a substantial enhancement in the electrical conductivity of gel nanocomposites, as discussed in Section 3.3. It is well understood that the chemistry of the filler particle surface plays an important role in ion–surface interactions and also has an impact on ion transport in composite electrolytes. As mentioned in Section 3.1, the SiO_2 filler particles in the present case belong to acidic oxides. The surface charges on these silica particles loosely bind anions (ClO_4^-) and free up cations. This is a possible reason for the slight enhancement in the Na^+ ion transport number. On the other hand, the surface charges on silica particles also provide sites for the conduction of loosely bound anions within the space-charge region formed between silica particles and the gel electrolyte. The enhancement in the overall electrical conductivity is due to the slight enhancement in the cationic charge carriers and a predominant increase in the anionic mobility due to the presence of SiO_2 nanoparticles.

4. Conclusions

PMMA-based, sodium ion conducting, gel polymer electrolyte nanocomposite films dispersed with SiO_2 nanoparticles have been synthesised and characterized. From structural, thermal, electrical and electrochemical studies, the following conclusions can be drawn.

(i) SEM and XRD studies confirm the composite nature of the gel polymer electrolyte films.
(ii) Ion–filler-polymer interactions play an important role in the ionic transport of the gel polymer electrolyte nanocomposite films, as found from FTIR spectroscopic studies.

(iii) Nanocomposites offer optimized conductivity ($\sigma \sim 3.4 \times 10^{-3}\,S\,cm^{-1}$ at 20 °C) with a sufficiently wider electrochemical potential window and good thermal stability of the gel-phase over the temperature range of −80 to 140 °C.
(iv) An electrochemical equilibrium between the sodium electrode and the Na^+ ion has been established from cyclic voltammetric studies, and hence Na^+ ion conduction in gel nanocomposite has been confirmed.
(v) A slight enhancement in the sodium ion transport number is observed due to the dispersion of SiO_2 nanoparticles in the gel system. The enhancement in electrical conductivity is explained in terms of interaction between anions and the filler surface.
(vi) The optimized gel nanocomposite appears to be an excellent substitute for liquid electrolytes in various ionic devices that include rechargeable sodium batteries and supercapacitors/ultracapacitors.

Acknowledgements

The authors acknowledge the financial support received from the University Grant Commission, New Delhi [Sanction No.: F.31–20/2005 (SR)] and the University of Delhi (under the Scheme to strengthen R&D Doctoral Research Programme providing funds to University faculty, 11-17 Research Fund, 2007). One author (DK) is grateful to CSIR (New Delhi) for the grant of Junior Research Fellowship.

References

[1] F. Groce, F. Gerace, G. Dautzemberg, S. Passerini, G.B. Appetecchi, B. Scrosati, Electrochim. Acta 39 (2004) 2187–2194.
[2] T. Michot, A. Nishimoto, M. Watanabe, Electrochim. Acta 45 (2000) 1347–1360.
[3] M. Stephan, Eur. Polym. J. 42 (2006) 21–42.
[4] R.C. Agrawal, G.P. Pandey, J. Phys. D: Appl. Phys. 41 (2008) 223001–223018.
[5] J. Jiang, D. Gao, Z. Li, G. Su, React. Funct. Polym. 66 (2006) 1141–1148.
[6] C. Capiglia, Y. Saito, H. Kataoka, T. Kodama, E. Quartarone, P. Mustarelli, Solid State Ionics 131 (2000) 291–299.
[7] B. Singh Lalia, N. Yoshimoto, M. Egashira, M. Morita, J. Power Sources 194 (2009) 531–535.
[8] T. Sato, K. Banno, T. Maruo, R. Nozu, J. Power Sources 152 (2005) 264–271.
[9] G.P. Pandey, S.A. Hashmi, J. Power Sources 187 (2009) 627–634.
[10] C. Sirisopanaporn, A. Fernicola, B. Scrosati, J. Power Sources 186 (2009) 490–495.
[11] M. Wachtler, D. Ostrovskii, P. Jacobsson, B. Scrosati, Electrochim. Acta 50 (2004) 357–361.
[12] V. Gentili, S. Panero, P. Reale, B. Scrosati, J. Power Sources 170 (2007) 185–190.
[13] X.-L. Wang, Q. Cai, L.-Z. Fan, T. Hua, Y.-H. Lin, C.-W. Nan, Electrochim. Acta 53 (2008) 8001–8007.
[14] C.-M. Yang, H.-S. Kim, B.-K. Na, K.-S. Kum, B.W. Cho, J. Power Sources 156 (2006) 574–580.
[15] B. Kumar, J. Power Sources 135 (2004) 215–231.
[16] B. Kumar, S. Nellutla, J.S. Thokchom, C. Chen, J. Power Sources 160 (2006) 1329–1335.
[17] S. Ahmad, S. Ahmad, S.A. Agnihotry, J. Power Sources 140 (2005) 151–156.
[18] G.P. Pandey, R.C. Agrawal, S.A. Hashmi, J. Power Sources 190 (2009) 563–572.
[19] Y.-J. Wang, D. Kim, Electrochim. Acta 52 (2007) 3181–3189.
[20] M. Walkowiak, A. Zalewska, T. Jesionowski, M. Pokora, J. Power Sources 173 (2007) 721–728.
[21] D. Saikia, A. Kumar, Eur. Polym. J. 41 (2005) 563–568.
[22] Y. Liu, J.Y. Lee, L. Hong, J. Power Sources 129 (2004) 303–311.
[23] J.-M. Tarascon, A.S. Gozdz, C.N. Schmutz, F.K. Shokoohi, P.C. Warren, Solid State Ionics 86–88 (1996) 49–54.
[24] G.B. Appetecchi, P. Romagnoli, B. Scrosati, Electrochem. Commun. 3 (2001) 281–284.
[25] N. Byrne, J. Efthimiadis, D.R. MacFarlane, M. Forsyth, J. Mater. Chem. 14 (2004) 127–133.
[26] G.G. Kumar, S. Sampath, Solid State Ionics 160 (2003) 289–300.
[27] S.A. Hashmi, A.K. Thakur, H.M. Upadhyaya, Eur. Polym. J. 34 (1998) 1277–1282.
[28] R.M. Dell, Solid State Ionics 134 (2000) 139–158.
[29] D.A.J. Rand, R. Woods, R.M. Dell, Batteries for Electric Vehicles, Wiley, 1998, p. 328.
[30] R. Kumara, A. Subramania, N.T. Kalyana Sundaram, G. Vijaya Kumar, I. Baskaran, J. Membr. Sci. 300 (2007) 104–110.
[31] S.A. Hashmi, Ashok Kumar, S.K. Tripathi, J. Phys. D: Appl. Phys. 40 (2007) 6527–6534.
[32] S.A. Hashmi, S. Chandra, J. Mater. Sci. Eng. B 34 (1995) 18–26.
[33] J. Evans, C.A. Vincent, P.G. Bruce, Polymer 28 (1987) 2324–2328.
[34] A.K. Thakur, S.A. Hashmi, to be published.
[35] J. Zhou, P.S. Fedkiw, Solid State Ionics 166 (2004) 275–293.
[36] J.P. Sharma, S.S. Sekhon, Solid State Ionics 178 (2007) 439–445.
[37] B.K. Choi, K. Shin, Solid State Ionics 86–88 (1996) 303–306.
[38] S.A. Hashmi, H.M. Upadhayaya, A.K. Thakur, in: B.V.R. Chowdari, W. Wang (Eds.), Solid State Ionics: Materials and Devices, World Scientific, Singapore, 2000, p. 461.
[39] G.P. Pandey, S.A. Hashmi, R.C. Agrawal, Solid State Ionics 179 (2008) 543–549.
[40] M.A. Ratner, in: J.R. MacCallum, C.A. Vincent (Eds.), Polymer Electrolyte Reviews 1, Elsevier Applied Science, London and New York, 1987, p. 173.